

Cardiotoxicity induced by the combination therapy of chloroquine and azithromycin in human embryonic stem cell-derived cardiomyocytes

Ye Seul Kim^{1,#}, Soo Yong Lee^{2,#}, Jung Won Yoon¹, Dasol Kim¹, Sangbin Yu¹, Jeong Su Kim^{2,*} & Jae Ho Kim^{1,*}

¹Department of Physiology, School of Medicine, Pusan National University, Yangsan 50612, ²Division of Cardiology, Department of Internal Medicine and Research Institute for Convergence of Biomedical Science and Technology, Pusan National University Yangsan Hospital, Pusan National University School of Medicine, Yangsan 50612, Korea

Combination therapy using chloroquine (CQ) and azithromycin (AZM) has drawn great attention due to its potential anti-viral activity against SARS-CoV-2. However, clinical trials have revealed that the co-administration of CQ and AZM resulted in severe side effects, including cardiac arrhythmia, in patients with COVID-19. To elucidate the cardiotoxicity induced by CQ and AZM, we examined the effects of these drugs based on the electrophysiological properties of human embryonic stem cell-derived cardiomyocytes (hESC-CMs) using multi-electrode arrays. CQ treatment significantly increased the field potential duration, which corresponds to prolongation of the QT interval, and decreased the spike amplitude, spike slope, and conduction velocity of hESC-CMs. AZM had no significant effect on the field potentials of hESC-CMs. However, CQ in combination with AZM greatly increased the field potential duration and decreased the beat period and spike slope of hESC-CMs when compared with CQ monotherapy. In support of the clinical data suggesting the cardiovascular side effects of the combination therapy of CQ and AZM, our results suggest that AZM reinforces the cardiotoxicity induced by CQ in hESC-CMs. [BMB Reports 2020; 53(10): 545-550]

INTRODUCTION

Coronavirus disease 2019 (COVID-19), a pandemic declared by the World Health Organization, has become a major global

health concern. Large-scale efforts have been undertaken globally to develop safe and effective vaccines and therapeutics against COVID-19. Chloroquine (CQ) and hydroxychloroquine (HCQ) are drugs that are widely used in the treatment of malaria and chronic inflammatory diseases, including rheumatoid arthritis and systemic lupus erythematosus. Recently, the anti-viral potential of CQ/HCQ has also been reported (1-3). CQ/HCQ has been reported to inhibit *Coronaviridae* (including SARS and SARS-CoV-2) *in vitro*, suggesting the potential use of these drugs in the treatment of COVID-19 (4, 5). In addition, a clinical study has reported 100% viral clearance in the nasopharyngeal swabs of six patients with COVID-19 after combination therapy with HCQ and azithromycin (AZM) (6). Therefore, CQ/HCQ is considered an attractive drug for treatment of COVID-19 (5, 7, 8). However, accumulating evidence suggests that CQ/HCQ does not provide any clinical benefits in alleviating the disease severity and progression in patients with COVID-19 (9, 10). Moreover, HCQ is not effective for post-exposure prophylaxis of COVID-19 (11), and therefore, the focus on CQ/HCQ as a treatment option is decreasing. The U.S. Food and Drug Administration revoked its emergency use authorization and warned of the potentially deadly side effects of CQ/HCQ.

Both CQ and HCQ have been reported to interfere with ventricular repolarization, leading to prolongation of the corrected QT interval and an increased risk of torsades de pointes (12, 13). AZM, one of the frequently used macrolides, is known to exert anti-viral/bacterial and immunomodulatory effects, including anti-inflammatory effects (14, 15). Several reports have suggested a possible synergistic effect of the combination of HCQ and AZM, thereby prompting their use in combination (16, 17). However, recent clinical studies have reported that the combination therapy of CQ/HCQ and AZM induces cardiotoxicity in patients (18, 19). Although AZM itself does not usually lead to clinically significant prolongation of the corrected QT interval (20), studies have shown that AZM in combination with CQ/HCQ induced QT interval prolongation and torsades de pointes in patients (21, 22). The cardiotoxic effects of CQ/HCQ and AZM are dose-dependent but

*Corresponding authors. Jae Ho Kim, Tel: +82-51-510-8073; Fax: +82-51-510-8076; E-mail: jhkimst@pusan.ac.kr; Jeong Su Kim, Tel: +82-55-360-1594; Fax: +82-55-360-2204; E-mail: j25ngsukim@gmail.com
#These authors contributed equally to this work.

<https://doi.org/10.5483/BMBRep.2020.53.10.165>

Received 9 August 2020, Revised 19 August 2020,
Accepted 26 August 2020

Keywords: Cardiomyocytes, Cardiotoxicity, Chloroquine, COVID-19, Embryonic stem cells

can vary among individuals (23), suggesting the need to elucidate the cardiotoxicity of CQ/HCQ and AZM *in vitro* using cardiomyocytes.

Analysis of cardiotoxicity is generally conducted in non-cardiac cells that overexpress specific ion channels or in *in vivo* animal models. However, these traditional methods for screening of cardiotoxicity are hampered by their inability to accurately predict cardiotoxicity, primarily due to species-specific differences and the lack of cardiomyocyte-specific signaling components in these systems (24). The lack of a human cardiomyocyte cell line and the difficulties in preparing primary human cardiomyocytes have been major impediments to drug development and analysis of cardiotoxicity. Human pluripotent stem cells, including embryonic stem cells and induced pluripotent stem cells, have been utilized to produce functional cardiomyocytes, which are highly useful in disease modeling, drug screening, and cardiotoxicity testing (25-27).

To ascertain the cardiotoxicity of CQ/HCQ combination therapy and AZM observed in clinical trials, we investigated the effects of these drugs on the electrophysiological properties of human embryonic stem cell-derived cardiomyocytes (hESC-CMs) using multi electrode arrays (MEA).

RESULTS

Chloroquine treatment induces cardiac arrhythmia in hESC-CMs

The effects of CQ on cardiotoxicity were investigated by treating hESC-CMs with CQ or control vehicle, i.e., dimethyl sulfoxide (DMSO) for 6 h, followed by measurement of field potentials using MEA. As shown in Fig. 1A, the typical field potential waveforms of hESC-CMs were exposed to 0.1% DMSO or 5 μ M CQ. CQ treatment increased FPD (Field Potential Duration), the *in vitro* analog of the QT interval, measured from the initial Na^+ spike to the maxima of the K^+ repolarization wave, in a time-dependent manner. FPD correlates with action potential duration in *in vitro* patch-clamp studies (28, 29). Conversely, CQ treatment decreased the spike slope and the spike amplitude in a time-dependent manner (Fig. 1B-D). We also analyzed the dose-dependent effects of CQ on the electrical properties of hESC-CMs. BP (Beat Period) was not significantly affected by increasing the CQ dose up to 5 μ M (Fig. 1E). However, FPD was significantly augmented in response to treatment with 1 μ M CQ, and the CQ-induced increase in FPD was sustained up to 5 μ M CQ (Fig. 1F). Spike amplitude and spike slope were significantly decreased by treatment with 5 μ M CQ (Fig. 1G and 1H). Furthermore, the conduction velocity of hESC-CM was inhibited by CQ in a dose-dependent manner (Fig. 1I). These results suggest that CQ affects the electrophysiological properties of hESC-CMs, resulting in cardiac arrhythmia.

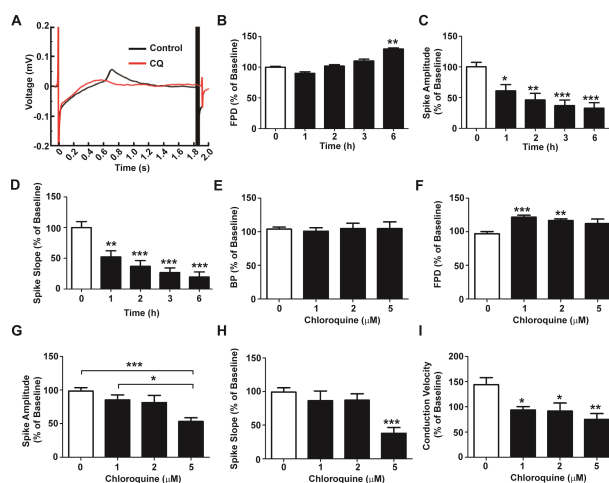


Fig. 1. Effects of chloroquine (CQ) on the electrical properties of hESC-CMs. (A) Representative field potential duration (2 s) of hESC-CMs treated with 5 μ M CQ or control vehicle. (B-D) Time-dependent effects of CQ on field potential duration (B), spike amplitude (C), and spike slope (D) of hESC-CMs. (E-I) Dose-dependent effects of CQ on beat period (E), field potential duration (F), spike amplitude (G), spike slope (H), and conduction velocity (I) of hESC-CMs. Data are expressed as mean \pm S.D. (n = 4). *P < 0.05, **P < 0.01, ***P < 0.001.

Azithromycin treatment does not alter the electrical properties of hESC-CMs

To examine the effects of AZM on the electrical properties of hESC-CMs, hESC-CMs were treated with AZM or control vehicle for 6 h, followed by the measurement of field potentials using MEA. Fig. 2A shows the typical field potential waveforms of hESC-CMs exposed to control vehicle or 5 μ M AZM. AZM treatment did not significantly affect FPD, spike slope, or spike amplitude for 6 h (Fig. 2B-D). In addition, we treated hESC-CMs with AZM at doses corresponding to different levels of AZM toxicity in clinical settings, and analyzed the dose-dependent effects of AZM on the electrical properties of hESC-CMs. BP, FPD, spike amplitude, spike slope, and conduction velocity of hESC-CMs were not affected by increasing the dose of AZM up to 5 μ M (Fig. 2E-I). These results suggest that AZM treatment did not affect the electrophysiological properties of hESC-CMs.

Combination therapy of CQ and AZM induces cardiac arrhythmia and QT prolongation

We investigated the field potentials of hESC-CM after co-treatment with CQ and AZM to investigate the effects of combination therapy of CQ and AZM on QT prolongation and subsequent cardiac complication. Fig. 3A shows the typical field potential waveforms of hESC-CM exposed to control vehicle or 5 μ M AZM + 5 μ M CQ (Fig. 3A). Monotherapy with either CQ or AZM had no effect on the BP of hESC-CMs, whereas combination therapy of CQ and AZM significantly reduced the BP

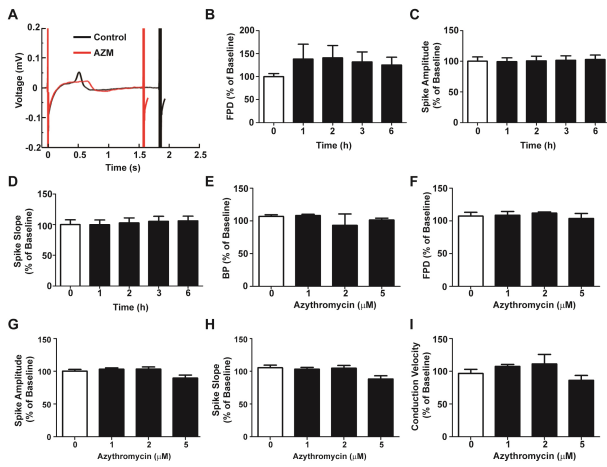


Fig. 2. Effects of azithromycin (AZM) on the electrical properties of hESC-CMs. (A) Representative field potential duration (2 s) of hESC-CMs treated with 5 μ M AZM or control vehicle. (B-D) Time-dependent effects of AZM on field potential duration (B), spike amplitude (C), and spike slope (D) of hESC-CMs. (E-I) Dose-dependent effects of AZM on beat period (E), field potential duration (F), spike amplitude (G), spike slope (H), and conduction velocity (I) of hESC-CMs. Data are expressed as mean \pm S.D. (n = 4). *P < 0.05, **P < 0.01, ***P < 0.001.

of hESC-CMs (Fig. 3B). Moreover, CQ monotherapy slightly increased FPD, and combination therapy of CQ and AZM greatly potentiated the FPD of hESC-CMs (Fig. 3C). Spike amplitude and spike slope of hESC-CMs were more potently inhibited by the combination therapy of CQ and AZM compared with CQ monotherapy (Fig. 3D and 3E). Furthermore, the conduction velocity of hESC-CMs was also inhibited by CQ monotherapy; however, the combination therapy of CQ and AZM did not potentiate the CQ-induced inhibition of conduction velocity (Fig. 3F). These findings are consistent with previous studies and clinical trials showing a correlation between CQ treatment with or without AZM and cardiovascular defects.

DISCUSSION

The key findings of the present study can be summarized as follows: CQ monotherapy induced cardiac arrhythmia in hESC-CMs in a dose-dependent manner; AZM monotherapy did not alter the electrophysiological properties of hESC-CMs; and combination therapy with CQ and AZM potentiated QT prolongation and cardiac arrhythmia in hESC-CMs without affecting cell viability of hESC-CM (Supplementary Fig. 1). Recently, CQ and HCQ were found to decrease viral replication in a dose-dependent manner in SARS-CoV-2-infected Vero cells *in vitro*, and the EC₅₀ value for CQ was 5.47 μ M at 48 h (5). In the present study, we demonstrated that hESC-CMs treated with 5 μ M CQ exhibited a time-dependent increase in FPD and spike slope,

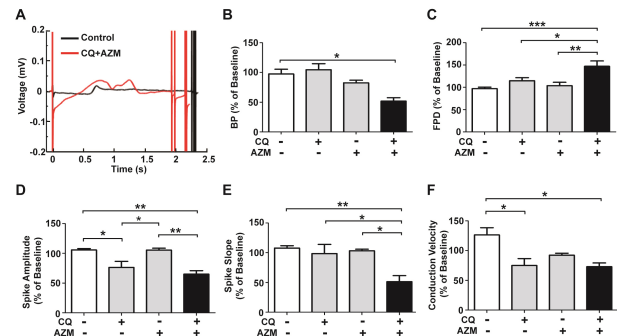


Fig. 3. Effects of combination therapy comprising chloroquine (CQ) and azithromycin (AZM) on hESC-CMs. (A) Representative field potential duration (2.5 s) of hESC-CMs treated with 5 μ M CQ+ 5 μ M AZM or control vehicle. (B-F) Effects of CQ and AZM combination therapy on beat period (B), field potential duration (C), spike amplitude (D), spike slope (E), and conduction velocity (F) of hESC-CMs. Data are expressed as mean \pm S.D. (n = 4). *P < 0.05, **P < 0.01, ***P < 0.001.

and a time-dependent decrease in spike amplitude. Additionally, the combination therapy of 5 μ M CQ and 5 μ M AZM significantly increased FPD when compared with CQ monotherapy. In the severe form of disseminated viremia, SARS-CoV-2 has been reported to affect the myocardium and cause non-ischemic myocardial injury, including myocarditis (30-32). In this case, the myocardium becomes unstable, leading to QT prolongation; therefore, selection of less cardiotoxic drugs is necessary for the treatment of COVID-19.

CQ is known to block hERG 1A and 1A/1B potassium channels underlying the repolarizing potassium current I_{Kr} in the heart (33, 34). CQ also binds to cardiac sodium, calcium, and inwardly-rectifying potassium channels to induce QRS widening and cardiac conduction abnormalities (35). In a recent review of cardiac complications attributed to long-term CQ/HCQ use, cardiac conduction disorders and heart failure were the most common complications (12). In the comprehensive *in vitro* proarrhythmia assay initiative using human induced pluripotent stem cell-derived cardiomyocytes for testing of drug-induced risk of torsades de pointes, CQ has been shown to induce QT prolongation as well as mild PR and QRS widening (36). Additionally, CQ has a relatively narrow therapeutic window, with multiple cases of overdose leading to death from hemodynamic collapse or ventricular arrhythmias. A lethal overdose has recently been observed in patients with COVID-19. While the ability of CQ/HCQ to prolong the QT interval does not appear to be associated with a substantial risk of sudden cardiac arrest or torsades de pointes (37), in the present study, we demonstrated that AZM reinforced the cardiotoxicity induced by CQ. Therefore, cardiotoxicity tests must be performed before treatment with CQ/HCQ in clinical settings, as most clinical trials so far have not included patients with cardiovascular comorbidities or diseases associated with

the greatest risk of arrhythmia, such as COVID-19.

In summary, CQ monotherapy or combination therapy of CQ and AZM affected the electrophysiological properties of hESC-CMs prone to arrhythmogenic status. Therefore, the evaluation of cardiotoxicity induced by drugs used for the novel treatment of COVID-19 should be made. The use of hESC-CMs and MEA for the determination of cardiotoxicity provides rapid and comprehensive dose-related information obviating the need for animal studies.

MATERIALS AND METHODS

Materials

Dulbecco's modified Eagle medium (DMEM)/F12, glucose-free DMEM, Roswell Park Memorial Institute (RPMI) 1640 medium, fetal bovine serum (FBS), penicillin/streptomycin, collagenase type IV, dispase, accutase, B27 supplement, B27 supplement minus insulin, and 0.05% trypsin-ethylenediaminetetraacetic acid (trypsin-EDTA) were purchased from Thermo Fisher Scientific (Waltham, MA, United States). The mTeSR1 and mTeSR1 5× supplements were purchased from STEMCELL Technologies Inc. (Vancouver, BC, Canada). Human embryonic stem cell line H9 (WA09) was procured from WiCell Research Institute (Madison, WI, United States). Matrigel (#354277) was supplied by Corning Life Sciences (Tewksbury, MA, United States). Mitomycin C, gelatin, Y27632, CQ phosphate, AZM, and all other unlisted reagents were acquired from Sigma-Aldrich (St. Louis, MO, United States).

Culture of human embryonic stem cells (hESCs)

Mouse embryonic fibroblasts (MEFs) were purchased from CEF Corporation (www.cefobio.com, Seoul, Korea). Feeders were prepared by treating MEFs after passage 5 with 5 ng/ml mitomycin C for 1.5 h and seeded at a concentration of 4×10^5 cells/60 mm dish (0.1% gelatin coated) in DMEM containing 10% FBS and penicillin/streptomycin (125 U/ml). Undifferentiated H9 hESC colonies were cultured on mitomycin C-treated non-mitogenic MEF feeder layer. H9 hESC colonies were maintained in DMEM/F12 medium containing $1 \times$ GlutaMAX, penicillin/streptomycin (125 U/ml), β -mercaptoethanol (60 μ M), $1 \times$ NEAA (#11140, Thermo Fisher Scientific), 20% KSR medium (#10828, Thermo Fisher Scientific), and basic fibroblast growth factor (5 ng/ml) (#100-18B, PeproTech, Rocky Hill, NJ) for 4 days; the medium was changed daily. H9 hESC colonies were passaged on day 5 by treatment with the dissociation medium (DMEM/F12 containing 200 μ g/ml collagenase type IV and 1 mg/ml dispase) for 12 min. Next, the cells were harvested via sedimentation and washed twice with maintenance medium. The collected hESC colonies were sliced into fragments of 50-80 μ m diameter with a pipette and plated onto MEF feeders at a ratio of 1:3 or 1:4, followed by incubation at 37°C under 5% CO₂ atmosphere. The study protocol was approved by the Public Institutional Bioethics Committee designated by the MOHW (P01-201410-ES-02). All experiments

were performed in accordance with relevant guidelines and regulations.

Differentiation of hESCs into cardiomyocytes

For differentiation of H9 hESCs into cardiomyocytes, single cell suspension of hESCs was prepared by treating hESCs with accutase at 37°C for 7 to 8 min. The single cell suspension was seeded in Matrigel-coated 6-well culture plates prepared as described previously (38, 39). In brief, the dissociated cells were plated in mTeSR1 medium supplemented with Y27632 (5 μ M) at a density of 1.4×10^6 cells/well. The medium was replaced every day for 3 days until 80-90% confluence was obtained. To initiate differentiation, the medium was changed to RPMI/B27 minus insulin medium containing the GSK3-specific inhibitor CHIR99021 (10 μ M; Selleck Chemicals, Houston, TX). The cells were incubated in this medium for 24 h (day 0), followed by incubation in RPMI/B27 minus insulin medium for 48 h (day 1-3). The differentiating cells were incubated in RPMI/B27 minus insulin medium containing the Wnt signaling inhibitor IWP2 (5 μ M; Tocris Bioscience, Bristol, United Kingdom) for 48 h (day 3-5). The culture medium was replaced on days 5 and 7 with fresh RPMI/B27 minus insulin medium. The culture medium was replaced with fresh RPMI/B27 medium between days 8 and 20, once every 3 days. The cells were incubated in a humidified incubator at 37°C under 5% CO₂ atmosphere. In the final phase of cardiomyocyte differentiation, i.e., on day 20, the medium was replaced with glucose-free DMEM supplemented with lactate (4 mM) as described previously (40). Differentiating hESCs were treated with 0.05% trypsin-EDTA at 37°C for 5 min to obtain a single cell suspension. The cells were collected in RPMI medium supplemented with 20% FBS, and seeded onto a 0.1% gelatin-coated dish containing RPMI medium supplemented with B27.

Microelectrode array measurements

The electrophysiological properties of hESC-CM were measured using the Maestro MEA system (Maestro EDGE, Axion Biosystems, Atlanta, United States) with 16 electropolymerized poly(3,4-ethylenedioxythiophene) (PEDOT) electrodes per well. Detailed methods of MEA analysis are described in the supporting information.

Statistical analyses

All data are presented as mean \pm SD. We used analysis of variance (ANOVA) with *posthoc* tests to compare more than two independent samples or experimental groups. All other statistical tests were performed using the GraphPad Prism statistics software.

ACKNOWLEDGEMENTS

This study was supported by research grants (NRF-2015R1A5A2009656, NRF-2015M3A9C6030280, and NRF-2017M3A9B4051542) of the National Research Foundation of Korea (NRF)

funded by the Ministry of Education, Science, and Technology.

CONFLICTS OF INTEREST

The authors have no conflicting interests.

REFERENCES

1. Savarino A, Boelaert JR, Cassone A, Majori G and Cauda R (2003) Effects of chloroquine on viral infections: an old drug against today's diseases? *Lancet Infect Dis* 3, 722-727
2. Savarino A, Di Trani L, Donatelli I, Cauda R and Cassone A (2006) New insights into the antiviral effects of chloroquine. *Lancet Infect Dis* 6, 67-69
3. Vincent MJ, Bergeron E, Benjannet S et al (2005) Chloroquine is a potent inhibitor of SARS coronavirus infection and spread. *Virology* 339, 243-250
4. Wang M, Cao R, Zhang L et al (2020) Remdesivir and chloroquine effectively inhibit the recently emerged novel coronavirus (2019-nCoV) in vitro. *Cell Res* 30, 269-271
5. Yao X, Ye F, Zhang M et al (2020) In Vitro Antiviral Activity and Projection of Optimized Dosing Design of Hydroxychloroquine for the Treatment of Severe Acute Respiratory Syndrome Coronavirus 2 (SARS-CoV-2). *Clin Infect Dis* 71, 732-739
6. Gautret P, Lagier JC, Parola P et al (2020) Hydroxychloroquine and azithromycin as a treatment of COVID-19: results of an open-label non-randomized clinical trial. *Int J Antimicrob Agents* 56, 105949
7. Colson P, Rolain JM and Raoult D (2020) Chloroquine for the 2019 novel coronavirus SARS-CoV-2. *Int J Antimicrob Agents* 55, 105923
8. Satarker S, Ahuja T, Banerjee M et al (2020) Hydroxychloroquine in COVID-19: Potential mechanism of action against SARS-CoV-2. *Curr Pharmacol Rep* 6, 203-211
9. Das S, Bhowmick S, Tiwari S and Sen S (2020) An Updated Systematic Review of the Therapeutic Role of Hydroxychloroquine in Coronavirus Disease-19 (COVID-19). *Clin Drug Investig* 40, 591-601
10. Pillat MM, Kruger A, Guimaraes LMF et al (2020) Insights in chloroquine action: perspectives and implications in Malaria and COVID-19. *Cytometry A* 97, 872-881
11. Boulware DR, Pullen MF, Bangdiwala AS et al (2020) A Randomized Trial of Hydroxychloroquine as Postexposure Prophylaxis for Covid-19. *N Engl J Med* 383, 517-525
12. Chatre C, Roubille F, Vernhet H, Jorgensen C and Pers YM (2018) Cardiac Complications Attributed to Chloroquine and Hydroxychloroquine: A Systematic Review of the Literature. *Drug Saf* 41, 919-931
13. White NJ (2007) Cardiotoxicity of antimalarial drugs. *Lancet Infect Dis* 7, 549-558
14. Min JY and Jang YJ (2012) Macrolide therapy in respiratory viral infections. *Mediators Inflamm* 2012, 649570
15. Tran DH, Sugamata R, Hirose T et al (2019) Azithromycin, a 15-membered macrolide antibiotic, inhibits influenza A (H1N1)pdm09 virus infection by interfering with virus internalization process. *J Antibiot (Tokyo)* 72, 759-768
16. Scherrmann JM (2020) Intracellular ABCB1 as a Possible Mechanism to Explain the Synergistic Effect of Hydroxychloroquine-Azithromycin Combination in COVID-19 Therapy. *AAPS J* 22, 86
17. Ohe M, Shida H, Jodo S et al (2020) Macrolide treatment for COVID-19: Will this be the way forward? *Biosci Trends* 14, 159-160
18. Chorin E, Dai M, Shulman E et al (2020) The QT interval in patients with COVID-19 treated with hydroxychloroquine and azithromycin. *Nat Med* 26, 808-809
19. Ramireddy A, Chugh H, Reinier K et al (2020) Experience With Hydroxychloroquine and Azithromycin in the Coronavirus Disease 2019 Pandemic: Implications for QT Interval Monitoring. *J Am Heart Assoc* 9, e017144
20. Juurlink DN (2014) The cardiovascular safety of azithromycin. *CMAJ* 186, 1127-1128
21. Mitra RL, Greenstein SA and Epstein LM (2020) An algorithm for managing QT prolongation in coronavirus disease 2019 (COVID-19) patients treated with either chloroquine or hydroxychloroquine in conjunction with azithromycin: Possible benefits of intravenous lidocaine. *Heart Rhythm Case Rep* 6, 244-248
22. Ray WA, Murray KT, Hall K, Arbogast PG and Stein CM (2012) Azithromycin and the risk of cardiovascular death. *N Engl J Med* 366, 1881-1890
23. Juurlink DN (2020) Safety considerations with chloroquine, hydroxychloroquine and azithromycin in the management of SARS-CoV-2 infection. *CMAJ* 192, E450-E453
24. Gintant G, Sager PT and Stockbridge N (2016) Evolution of strategies to improve preclinical cardiac safety testing. *Nat Rev Drug Discov* 15, 457-471
25. Satsuka A and Kanda Y (2020) Cardiotoxicity Assessment of Drugs Using Human iPS Cell-Derived Cardiomyocytes: Toward Proarrhythmic Risk and Cardio-Oncology. *Curr Pharm Biotechnol* 21, 765-772
26. Sharma A, McKeithan WL, Serrano R et al (2018) Use of human induced pluripotent stem cell-derived cardiomyocytes to assess drug cardiotoxicity. *Nat Protoc* 13, 3018-3041
27. Thomson JA, Itskovitz-Eldor J, Shapiro SS et al (1998) Embryonic stem cell lines derived from human blastocysts. *Science* 282, 1145-1147
28. Cheng DK, Tung L and Sobie EA (1999) Nonuniform responses of transmembrane potential during electric field stimulation of single cardiac cells. *Am J Physiol* 277, H351-362
29. Rast G, Weber J, Disch C, Schuck E, Ittrich C and Guth BD (2015) An integrated platform for simultaneous multiwell field potential recording and Fura-2-based calcium transient ratiometry in human induced pluripotent stem cell (hiPSC)-derived cardiomyocytes. *J Pharmacol Toxicol Methods* 75, 91-100
30. Inciardi RM, Lupi L, Zaccone G et al (2020) Cardiac Involvement in a Patient With Coronavirus Disease 2019 (COVID-19). *JAMA Cardiol* 5, 819-824
31. Sala S, Peretto G, Gramegna M et al (2020) Acute myocarditis presenting as a reverse Tako-Tsubo syndrome in a patient with SARS-CoV-2 respiratory infection. *Eur Heart J* 41, 1861-1862
32. Tavazzi G, Pellegrini C, Maurelli M et al (2020) Myocardial localization of coronavirus in COVID-19 cardiogenic shock. *Eur J Heart Fail* 22, 911-915
33. Sirenko O, Crittenden C, Callamaras N et al (2013)

- Multiparameter in vitro assessment of compound effects on cardiomyocyte physiology using iPSC cells. *J Biomol Screen* 18, 39-53
34. Traebert M, Dumotier B, Meister L, Hoffmann P, Dominguez-Estevez M and Suter W (2004) Inhibition of hERG K⁺ currents by antimalarial drugs in stably transfected HEK293 cells. *Eur J Pharmacol* 484, 41-48
 35. Mubagwa K (2020) Cardiac effects and toxicity of chloroquine: a short update. *Int J Antimicrob Agents* 56, 106057
 36. Vicente J, Zusterzeel R, Johannesen L et al (2019) Assessment of Multi-Ion Channel Block in a Phase I Randomized Study Design: Results of the CiPA Phase I ECG Biomarker Validation Study. *Clin Pharmacol Ther* 105, 943-953
 37. Haeusler IL, Chan XHS, Guerin PJ and White NJ (2018) The arrhythmogenic cardiotoxicity of the quinoline and structurally related antimalarial drugs: a systematic review. *BMC Med* 16, 200
 38. Lian X, Zhang J, Azarin SM et al (2013) Directed cardiomyocyte differentiation from human pluripotent stem cells by modulating Wnt/beta-catenin signaling under fully defined conditions. *Nat Protoc* 8, 162-175
 39. Lian X, Hsiao C, Wilson G et al (2012) Robust cardiomyocyte differentiation from human pluripotent stem cells via temporal modulation of canonical Wnt signaling. *Proc Natl Acad Sci U S A* 109, E1848-1857
 40. Tohyama S, Hattori F, Sano M et al (2013) Distinct metabolic flow enables large-scale purification of mouse and human pluripotent stem cell-derived cardiomyocytes. *Cell Stem Cell* 12, 127-137